VNU Journal of Science: Mathematics - Physics

Journal homepage: https://js.vnu.edu.vn/MaP

Original Article

Synthesis of Hydroxyapatite Coatings on Titanium Substrates by Plasma Electrolytic Oxidation

Vu Cong Manh[1], Dang Minh Duc[1], Le Van Toan[1,2], Ta Quoc Tuan[1,3], Le Thi Tam[1,3], Le Thi Bang[1,3], Nguyen Van Toan[1,3], Nguyen Ngoc Thang[1,3], Hoang Van Vuong[1,3], Cao Xuan Thang[1,3], Pham Hung Vuong[1,3,*]

[1]*School of Materials Science and Engineering, Hanoi University of Science and Technology (HUST), 1 Dai Co Viet, Hanoi, Vietnam*

[2]*Le Quy Don Technical University, 236 Hoang Quoc Viet, Hanoi, Vietnam*

[3]*Laboratory of Biomedical Materials, Hanoi University of Science and Technology (HUST), 1 Dai Co Viet, Hanoi, Vietnam*

Received 28th December 2025
Revised 20th March 2026; Accepted 28th April 2026

Abstract: In this study, hydroxyapatite (HA) coatings were synthesized on titanium substrates using the plasma electrolytic oxidation (PEO) technique to enhance corrosion resistance and improve the biocompatibility of implant materials. The experiments were conducted in an electrolyte containing calcium acetate hydrate and sodium dihydrogen phosphate monohydrate under a constant voltage of 500 V, with treatment durations of 1, 3, 5, and 7 minutes. The surface morphology and structural characteristics of the coatings were analyzed using various characterization techniques. X-ray diffraction (XRD) results revealed the distinct formation of hydroxyapatite phases when the treatment duration reached 7 minutes. Scanning electron microscopy (SEM) observations showed a uniformly porous surface morphology while energy-dispersive X-ray spectroscopy (EDS) confirmed the presence of calcium and phosphorus elements. Furthermore, corrosion performance evaluated in simulated body fluid (SBF) using Tafel polarization curves demonstrated that the PEO-coated samples exhibited significantly higher corrosion potentials and polarization resistance than bare titanium, indicating superior surface protection. *In vitro* cell culture experiments using BHK cells for 48 h and 72 h confirmed good cell attachment and proliferation on the HA-coated surfaces. These results demonstrate that hydroxyapatite coatings prepared by the plasma electrolytic oxidation method hold great potential for biomedical implant applications.

Keywords: Plasma electrolytic oxidation (PEO), titanium, hydroxyapatite, coating, biomedical.

* Corresponding author.
E-mail address: vuong.phamhung@hust.edu.vn

https//doi.org/10.25073/2588-1124/vnumap.5103

1. Introduction

Titanium and its alloys have become the standard materials in dental and orthopedic implants due to their exceptional combination of high mechanical strength, outstanding corrosion resistance, and good biocompatibility [1,2]. However, the titanium surface is inherently bioinert and does not form a direct chemical bond with bone tissue. This limitation can result in slow or incomplete osseointegration, thereby reducing the clinical performance and longevity of the implant [3]. Hydroxyapatite (HA, $Ca_{10}(PO_4)_6(OH)_2$), the principal inorganic component of bone and teeth, accounts for approximately 65-70% of the weight of natural bone. Owing to its structural and chemical similarity to bone minerals, HA exhibits excellent bioactivity and the ability to form direct chemical bonds with bone tissue, promoting adhesion, proliferation, and differentiation of osteogenic cells [4]. Nevertheless, HA is inherently brittle, with low mechanical strength and poor fatigue resistance, which limits its direct use in load-bearing implant applications [5]. A feasible and effective approach is to coat titanium substrates with HA, combining the mechanical robustness and corrosion resistance of titanium with the superior bioactivity of HA. This strategy enables the development of a composite system that harmoniously integrates mechanical and biological properties, fulfilling the requirements of biomedical applications [6].

Various techniques have been investigated to fabricate hydroxyapatite (HA) coatings on titanium substrates, including plasma spraying [7, 8], electrophoretic deposition (EPD) [9,10], sol-gel processing [11, 12], and biomimetic deposition in simulated body fluid (SBF) [13]. Nevertheless, conventional coating techniques still exhibit several inherent limitations, including insufficient interfacial bonding between the coating and the substrate [14-17], potential alterations in chemical composition due to processing conditions, and limited control over surface porosity and microstructural features.

Plasma electrolytic oxidation (PEO) has emerged as a particularly promising technique for an alternative surface modification approaches, as it enables the in situ formation of porous oxide coatings with strong metallurgical adhesion to the substrate, while simultaneously facilitating the incorporation of bioactive calcium-phosphate phases [18]. The PEO also known as micro-arc oxidation (MAO), is an advanced surface treatment technique capable of producing thick, porous, and strongly adherent oxide layers on light metals such as titanium and its alloys [19]. The process is carried out under high voltages that exceed the dielectric breakdown threshold of the native oxide film, resulting in microdischarge events on the electrode surface. The formation of hydroxyapatite (HA) coatings on titanium during the PEO process occurs through three fundamental stages. Initially, anodic oxidation produces a thin TiO_2 layer that serves as a dielectric barrier. As the voltage increases beyond the dielectric breakdown limit, this oxide layer is punctured, generating microplasma channels. Within these channels, temperatures can reach 2000-10000 K due to electron collisions and localized high pressure [20], leading to the melting and recrystallization of TiO_2, as well as enhanced ionic transport under the strong electric field. Calcium (Ca^{2+}) and phosphate (PO_4^{3-}) ions supplied from the electrolyte migrate into the molten oxide layer, where they undergo precipitation and transformation processes. In the alkaline, OH^--rich environment, the initial calcium phosphate phases form in amorphous or intermediate states and gradually rearrange and crystallize into HA. Parameters such as applied voltage, treatment duration, and electrolyte composition strongly influence the surface morphology, porosity, crystallinity, and phase composition of the coating. Higher voltages and longer treatment times generally increase the coating thickness and crystallinity, but may also cause overheating, electrolyte evaporation, and defect formation. Therefore, optimizing the processing parameters is crucial to obtain high-quality HA coatings that balance mechanical durability with enhanced bioactivity [21-23].

In recent years, numerous studies have focused on applying the plasma electrolytic oxidation (PEO) technique to deposit hydroxyapatite (HA) coatings on titanium and its alloys, with the aim of improving surface properties and enhancing the biocompatibility of implant materials. Reported results have shown that HA/Ti coatings not only increase surface hydrophilicity but also promote the adhesion, spreading,

and proliferation of osteogenic cells, while significantly reducing the time required for apatite formation during immersion in simulated body fluid (SBF) [24, 25]. However, most previous studies have required additional post-treatment steps after PEO - such as hydrothermal treatment [14, 17], sol-gel processing [26], heat treatment [27], or long-term immersion in SBF [28-30] - to achieve the formation of a fully developed HA phase.

In contrast to these previous approaches, this study demonstrates the direct synthesis of hydroxyapatite on titanium substrates via the PEO process at an applied voltage of 500 V, without the need for any additional post-treatment steps. This represents a significant distinction, as it simplifies the fabrication procedure, shortens processing time, and enhances the practical potential for producing biomedical implant components with greater cost-effectiveness and feasibility compared to conventional methods. To elucidate the formation mechanism and characteristics of the coating, plasma electrolytic oxidation was conducted in an electrolyte containing calcium acetate hydrate ($Ca(CH_3COO)_2$) and sodium dihydrogen phosphate monohydrate ($NaH_2PO_4 \cdot H_2O$) at different treatment durations. The resulting samples were comprehensively characterized using several advanced analytical techniques: scanning electron microscopy (SEM) to examine surface morphology, energy-dispersive X-ray spectroscopy (EDS) to identify elemental composition, and X-ray diffraction (XRD) to analyze crystalline phase formation. In addition, corrosion resistance was evaluated through Tafel polarization measurements. Notably, *in vitro* cell culture experiments using BHK cells for 48 h and 72 h revealed favorable cell adhesion and proliferation, confirming the promising potential of HA/Ti coatings produced by PEO for biomedical implant applications.

2. Materials and Methods

2.1. Synthesis of Hydroxyapatite Coatings by Plasma Electrolytic Oxidation

Commercially pure titanium (cp-Ti) sheets (Kahee Metal, South Korea) were cut into plates of 10 × 10 × 1 mm. Prior to plasma electrolytic oxidation (PEO), the titanium sheets were sequentially polished using 1000 grit and 2000 grit SiC sandpapers to obtain a uniform surface finish. The polished samples were then ultrasonically cleaned in acetone for approximately 10 minutes to remove surface contaminants, followed by rinsing with ethanol and deionized water, and dried prior to processing. The plasma electrolytic oxidation (PEO) treatment was carried out in an electrolyte solution containing calcium acetate hydrate ($Ca(CH_3COO)_2$, Merck, ≥ 95%) and sodium dihydrogen phosphate monohydrate ($NaH_2PO_4 \cdot H_2O$, Merck, ≥ 99%), which served as the sources of Ca^{2+} and PO_4^{3-} ions for hydroxyapatite formation. In the electrochemical system, the titanium sample was connected as the anode, a platinum rod was used as the cathode, and a direct current (DC) power supply was maintained at a constant voltage of 500 V. The formation of hydroxyapatite (HA) during plasma electrolytic oxidation process occurs as follows:

At the initial stage of oxidation, conventional anodic reactions occurred [31]:

$$Ti \rightarrow Ti^{4+} + 4e^- \quad (1)$$

$$Ti^{4+} + 2H_2O \rightarrow TiO_2 + 4H^+ \quad (2)$$

At the cathode, water reduction generated hydroxyl ions, leading to local alkalization:

$$2H_2O + 2e^- \rightarrow H_2\uparrow + 2OH^- \quad (3)$$

The initially formed TiO_2 layer acted as a dielectric barrier. When the applied voltage exceeded the dielectric breakdown potential of this oxide film, localized microplasma discharges were generated on the surface, producing transient high-temperature microzones that led to partial melting and rapid solidification of the oxide layer [32].

In the present electrolyte system, calcium acetate and sodium dihydrogen phosphate dissociate:

$$Ca(CH_3COO)_2 \rightarrow Ca^{2+} + 2CH_3COO^- \quad (4)$$

$$NaH_2PO_4 \rightarrow Na^+ + H_2PO_4^- \quad (5)$$

Under locally alkaline conditions induced by OH^- formation, phosphate species were progressively deprotonated to PO_4^{3-}:

$$H_2PO_4^- + OH^- \rightarrow HPO_4^{2-} + H_2O \quad (6)$$

$$HPO_4^{2-} + OH^- \rightarrow PO_4^{3-} + H_2O \quad (7)$$

Under the influence of the high voltage in the PEO process, these ions combine during the formation of TiO_2 to create ceramic compounds similar to HA, as described in the following reaction [32]:

$$10Ca^{2+} + 6PO_4^{3-} + 2OH^- \rightarrow Ca_{10}(PO_4)_6(OH)_2 \quad (8)$$

To investigate the effect of treatment duration, the samples were subjected to plasma electrolytic oxidation for four different time intervals: 1, 3, 5 and 7 minutes. Once the applied voltage exceeded the dielectric breakdown threshold, microplasma channels were generated, allowing Ca^{2+} and PO_4^{3-} ions to penetrate the TiO_2 layer and promote hydroxyapatite formation. During the process, the electrolyte temperature was maintained below 50 °C using a circulating cooling system to prevent rapid evaporation and ensure coating uniformity. After that, the samples were rinsed with deionized water and air-dried.

2.2. Characterization Methods

The treated samples were comprehensively characterized to evaluate surface morphology, phase structure, elemental composition, surface properties, and biocompatibility. The surface morphology and microstructure of the coatings were examined using scanning electron microscopy (SEM, JEOL JSM-IT200), while energy-dispersive X-ray spectroscopy (EDS) was employed to confirm the presence of calcium (Ca) and phosphorus (P) elements within the coatings. The crystalline structure was identified by X-ray diffraction (XRD, Bruker D8 Advance, Cu Kα, λ = 1.5406 Å), providing insight into the formation of hydroxyapatite and titanium oxide phases such as anatase and rutile.

The corrosion resistance was evaluated electrochemically in simulated body fluid (SBF) using a PGSTAT302N system (Metrohm Autolab) to obtain Tafel polarization curves, allowing comparison of surface protection performance between the untreated titanium and the PEO-treated samples. The corrosion current density (I_{corr}) and corrosion potential (E_{corr}) were determined by Tafel extrapolation of the anodic and cathodic branches of the polarization curves. The polarization resistance (R_p) was calculated using the equation 9 [33]:

$$R_p = \frac{\beta_a \times \beta_c}{2.303 \times I_{corr} \times (\beta_a + \beta_c)} \quad (9)$$

Where β_a and β_c represent the anodic and cathodic Tafel slopes, respectively. The corrosion rate (CR) was then determined from the corrosion current density according to Faraday's law:

$$CR = \frac{M}{n \times F} \times I_{corr} = 3.73 \times 10^{-4} \times \frac{M}{n} \times I_{corr} \quad (g/m^2h) \quad (10)$$

Where M is the molar mass of the metal (g/mol), n is the number of electrons involved in the corrosion reaction, and F is the Faraday constant.

The *in vitro* biocompatibility was examined through BHK cell culture on sterilized pure titanium and Ti/HA-coated samples. Cells were cultured in Dulbecco's Modified Eagle Medium (DMEM) supplemented with 10% fetal bovine serum (FBS) and 1% penicillin/streptomycin, under conditions of 37 °C and 5% CO_2. After 48 h and 72 h, the samples were collected and examined using SEM and fluorescence microscopy. Cells were stained with Phalloidin 555 to visualize the actin filament network

and DAPI to identify cell nuclei, enabling the assessment of cell adhesion, distribution, and proliferation on the coating surfaces.

3. Results and Discussion

The X-ray diffraction (XRD) patterns of the titanium substrate and the samples treated by PEO for 1, 3, 5 and 7 minutes are shown in figure 1. For the pure titanium sample, only the characteristic diffraction peaks of the α-Ti phase (ICDD 44-1294) were observed, confirming the high purity of the substrate material and the absence of impurities.

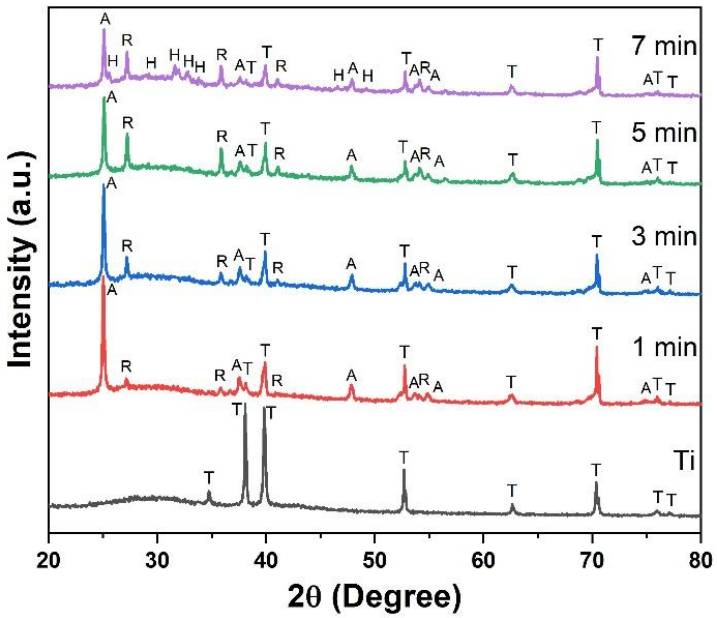
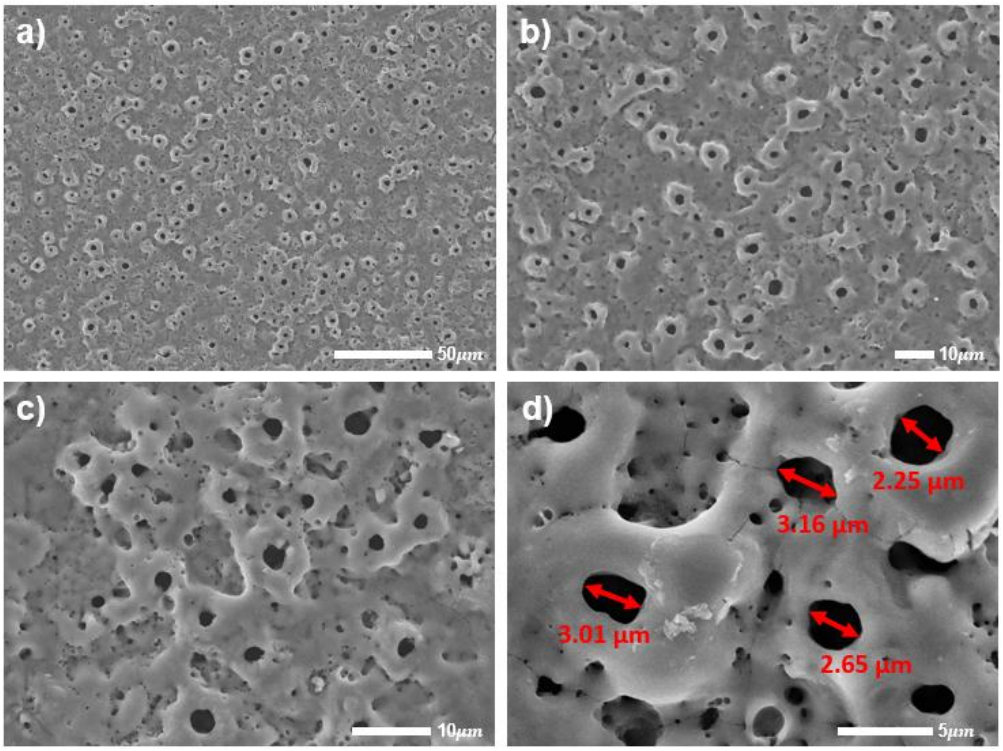


Figure 1. X-ray diffraction (XRD) patterns of Ti and HA/Ti coatings obtained at treatment times of 1, 3, 5, and 7 minutes, where T - Ti (ICDD 44-1294), A - TiO_2 anatase (ICDD 21-1272), R - TiO_2 rutile (ICDD 21-1276), and H - Hydroxyapatite (ICDD 09-0432).

After PEO treatment for 1 and 3 minutes, in addition to the Ti peaks, characteristic diffraction peaks of TiO_2 were detected in both anatase (ICDD 21-1272) and rutile (ICDD 21-1276) crystalline forms. For the sample treated for 5 minutes, several weak peaks appeared in the 2θ range of 31°-35°, which can be considered as initial signals indicating the formation of Ca-P phases or incompletely developed hydroxyapatite. Notably, after 7 minutes of treatment, distinct diffraction peaks corresponding to HA (ICDD 09-0432) were clearly observed at 25.9° (002), 28.9° (210), 31.7° (211), 32.2° (112), 32.9° (300), 34.0° (202), 46.7° (222), and 49.4° (213). The relative intensities of the Ti and TiO_2 peaks gradually decreased with increasing treatment time, mainly due to the shielding effect of a thicker and HA-enriched coating layer. These results indicate that treatment duration plays a crucial role in the HA formation mechanism while the short-duration PEO samples (1-3 minutes) primarily produced TiO_2 (anatase and rutile) and precursor Ca-P phases, well-crystallized hydroxyapatite was formed after 7 minutes. This finding demonstrates that the PEO method conducted in an electrolyte containing $Ca(CH_3COO)_2$ and $NaH_2PO_4 \cdot H_2O$ at 500 V can directly synthesize HA on titanium surfaces without the need for additional heat, hydrothermal, or long-term SBF treatments.

SEM observations (Figure 2) revealed that the HA/Ti coatings formed by the plasma process exhibited a typical multiscale porous structure. At a low magnification of 500×, the surface was densely covered with uniformly distributed micropores across the entire sample, forming a characteristic honeycomb-like morphology (Figure 2a). At higher magnifications of 1000-2000-5000×, pores with a wide range of sizes were observed, including numerous small pores in the submicron range (several hundred nanometers) together with larger discharge pores with diameters ranging from approximately 2.25 to 3.16 μm, as measured from the high-magnification SEM image (Figures 2b-d). This multiscale porous architecture is highly favorable for biomedical applications. Specifically, while macro-pores (>100 μm) are known to support bone ingrowth, micro-pores in the range of 1-10 μm play a crucial role in the early stages of osseointegration [34]. These pores increase the specific surface area and provide effective anchoring sites for cell filopodia, which typically possess diameters in the submicron range [25]. Furthermore, pores smaller than 10 μm promote the capillary-driven infiltration of biological fluids and the adsorption of adhesive proteins [26], facilitating robust cell attachment and proliferation as observed in the *in vitro* results (Figure 7). Many pores were surrounded by circular ridges with raised edges, which are characteristic features of localized melting and rapid solidification of the surface under plasma discharge (Figure 2d).

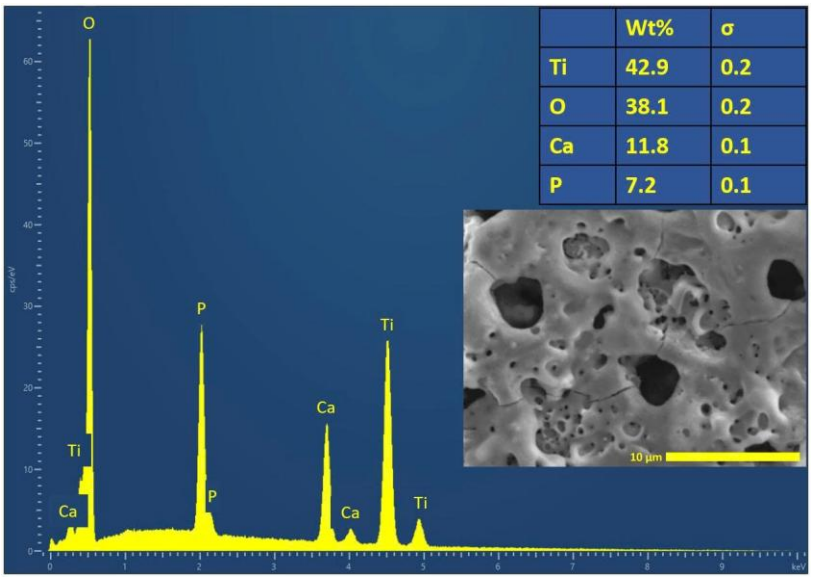


q

Figure 2. SEM results of the HA/Ti coating surface at different magnifications:
500× (a); 1000× (b); 2000× (c); 5000× (d).

Similar porous structures have been reported in previous studies. For example, Huang and Yoshimura reported that the pores formed on Sr-doped HA coatings prepared by electrochemical treatment ranged from 0.9 to 2.2 μm, depending on the applied voltage and treatment conditions [35]. Likewise, Durdu et al. observed that PEO coatings on Ti6Al4V exhibit micro-pores generated by discharge channels due to localized plasma reactions during oxidation [20]. Compared with these

studies, the slightly larger pore size observed in the present work may be attributed to the relatively high applied voltage of 500 V, which intensifies the plasma discharge energy and promotes the formation of larger discharge channels. The regions between pores showed relatively smooth recrystallized surfaces interspersed with fine roughened areas, along with submicron-sized spherical particles adhering to the pore edges and walls. These particle clusters correspond to hydroxyapatite incorporated into the coating via ion transport through plasma channels, consistent with the XRD results confirming HA phase formation at a treatment time of 7 minutes. This multiscale porous structure not only increases the effective surface area but also facilitates cell adhesion and allows body fluids to penetrate easily, thereby promoting biomineralization. In particular, the coexistence of micropores and HA particles is considered a key factor enhancing bioactivity, supporting cell attachment and spreading. This is further confirmed by the EDX analysis, which reveals the presence of calcium (Ca) and phosphorus (P) elements on the coating surface, as shown in figure 3.



	Wt%	σ
Ti	42.9	0.2
O	38.1	0.2
Ca	11.8	0.1
P	7.2	0.1

Figure 3. Elemental composition of the HA/Ti coating.

The EDS spectrum of the HA/Ti sample (Figure 3) shows that the obtained coating contains the main elements Ti, O, Ca and P, among which Ti (42.9 wt%) and O (38.1 wt%) are dominant, reflecting the presence of the titanium substrate and the oxide layer formed during the plasma electrolytic oxidation process. Notably, the appearance of Ca (11.8 wt%) and P (7.2 wt%) confirms that Ca-P co-deposition occurred on the surface, demonstrating the formation of a hydroxyapatite (HA)-rich or calcium phosphate-related coating. The calculated Ca/P ratio is approximately 1.64, which is close to the ideal value for HA (1.67), indicating that the resulting product tends to form a structure compatible with hydroxyapatite, although minor secondary phases or amorphous materials may still be present. Similar Ca/P ratios have been reported in previous studies on PEO-derived HA coatings. For instance, Durdu et al., reported Ca/P ratios close to the stoichiometric HA composition for coatings formed in Ca-P containing electrolytes during plasma electrolytic oxidation [20]. This similarity suggests that the coating produced in the present work tends to form hydroxyapatite or HA-like calcium phosphate phases, which are highly desirable for biomedical implant applications. The accompanying SEM images also reveal a typical porous surface with micro-sized pores, which not only increases the surface area

but also facilitates ion attachment and promotes the growth of biological apatite in simulated body fluid environments.

To further clarify the coating thickness and interfacial adhesion, cross-sectional SEM observations were conducted, as presented in figure 4. The HA/Ti coating exhibits a typical PEO-derived bilayer structure, consisting of a porous outer layer and a comparatively denser inner layer in direct contact with the titanium substrate. Thickness measurements taken at three representative positions reveal values of 14.16 µm, 12.39 µm, and 12.34 µm, corresponding to an average coating thickness of approximately 13 µm. The relatively small variation in thickness indicates good coating uniformity across the surface.

Importantly, the coating-substrate interface appears continuous and compact, with no observable cracks, voids, or delamination between the ceramic layer and the titanium substrate. The inner dense layer is tightly bonded to the substrate, suggesting strong interfacial integrity. This behavior is characteristic of plasma electrolytic oxidation coatings, which are formed through in situ anodic oxidation accompanied by localized microplasma discharges, leading to partial melting and metallurgical integration with the substrate. The absence of interfacial separation in the cross-sectional image provides direct microstructural evidence of excellent adhesion. Furthermore, the significant enhancement in corrosion resistance observed from the Tafel polarization measurements (Figure 6) indirectly confirms the structural stability and protective effectiveness of the coating.

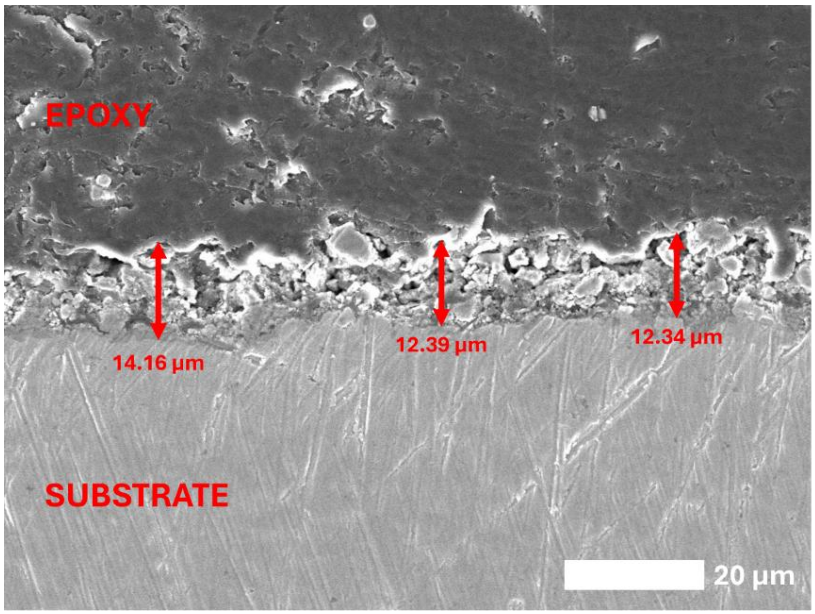


Figure 4. Cross-sectional SEM image of the HA/Ti coating.

Comparable coating thicknesses have been reported in previous studies on PEO coatings. For example, Huang and Yoshimura reported coating thicknesses in the range of 2.9-10.9 µm depending on the applied voltage during electrochemical surface treatment [35]. The slightly larger thickness obtained in the present study may be attributed to the higher applied voltage (500 V) and the continuous plasma discharge activity, which promotes faster oxide growth and ion incorporation. Compared with other PEO-derived coatings reported in previous studies, which may exhibit thinner oxide layers or noticeable interfacial transitions depending on electrolyte composition and dopant incorporation, the present HA/Ti coating shows a relatively thicker structure (~13 µm) with a clearly defined bilayer morphology [36,37]. By

contrast, the coating obtained in this study maintains a uniform thickness distribution and a continuous coating-substrate interface in the cross-sectional SEM image.

Figure 5 shows the current density-time (I-t) curve of the sample treated by the plasma electrolytic oxidation (PEO) method for 7 minutes at an applied voltage of 500 V. The results indicate that, in the initial stage, the current reached a peak value of approximately 1.65 A, reflecting the intense occurrence of plasma discharges at the onset of the process. Subsequently, the current rapidly decreased to around 0.8 A and remained fluctuating around this value throughout the treatment period.

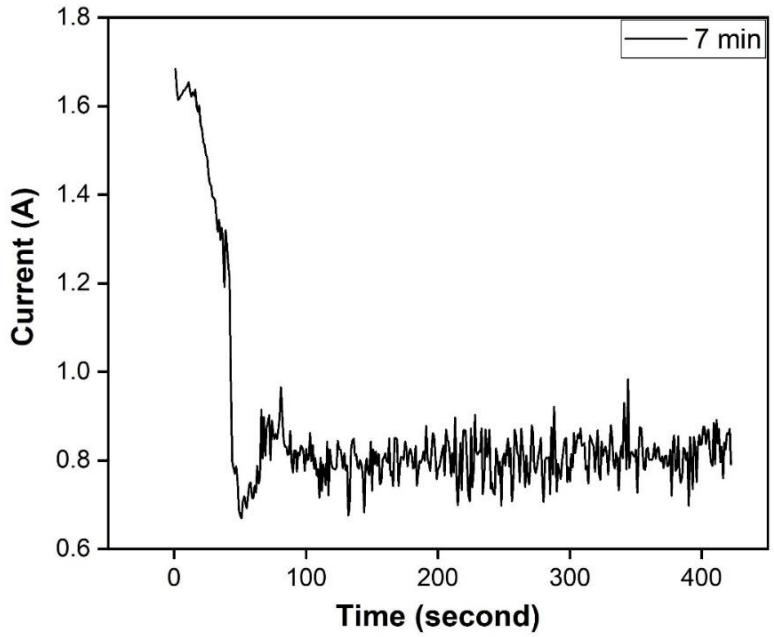


Figure 5. Current-time curve of the HA sample treated for 7 minutes.

The decrease in current over time is characteristic of the PEO process, as the oxide layer gradually thickens and becomes more insulating, thereby reducing the electrical conductivity of the sample surface. The small current fluctuations in the stable region indicate that micro-discharges continue to occur, sustaining the formation and redistribution of the oxide layer, which facilitates the crystallization and deposition of the HA phase on the surface. However, the relatively strong oscillations of the current during the steady stage suggest that the plasma system is not yet fully stable. This phenomenon may result from localized energy concentration of discharges, causing uneven temperature distribution on the surface and leading to alternating regions of intense and weak plasma activity. Such behavior can affect the uniformity of the coating, indicating that further optimization of the applied voltage or treatment time is needed to achieve higher plasma stability and a more homogeneous coating quality.

The Tafel polarization curves of the Ti substrate and the HA-coated Ti samples treated by the PEO process are presented in figure 6 and table 1. The results indicate that the Ti substrate exhibits a more negative corrosion potential (E_{corr} = 0.14878 V), a higher corrosion current density (I_{corr} = 2.5756×10^{-6} A/cm^2), a lower polarization resistance (R_p = 21700 Ω·cm^2), compared to that of the HA-coated sample, and a corrosion rate of 0.029928 mm/year, reflecting its limited corrosion resistance. In contrast, the HA-coated sample shows a positive shift in corrosion potential (E_{corr} = 0.76291 V), accompanied by a significant decrease in corrosion current density (I_{corr} = 0.49×10^{-6} A/cm^2) and a remarkable increase in polarization resistance (R_p = 61639 Ω·cm^2), compared to that of the bare Ti, resulting in a much lower

corrosion rate of only 0.0056938 mm/year, an improvement of over 80% compared to bare Ti. This outstanding enhancement is mainly attributed to the HA layer acting as a protective barrier that limits direct contact between the Ti substrate and the electrolyte, combined with the chemical stability and excellent biocompatibility of HA, thereby confirming the potential for biomedical applications.

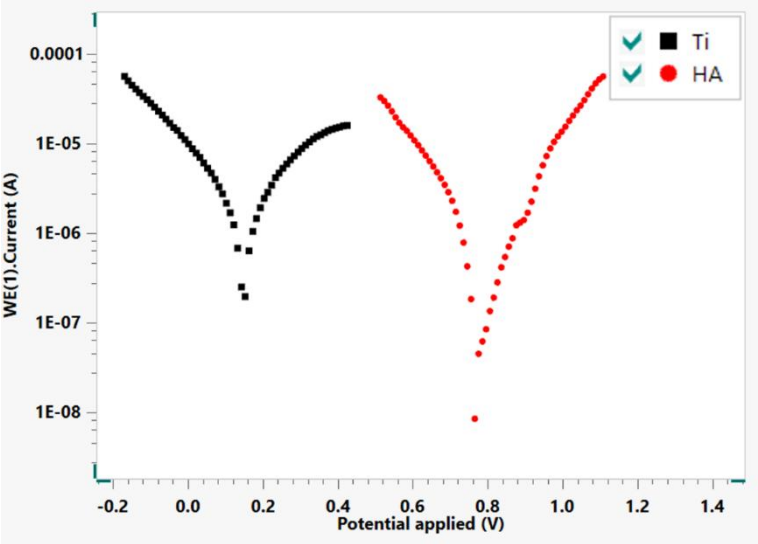


Figure 6. Tafel curves of the Ti sample and the HA coating.

Table 1. Electrochemical parameters from the Tafel curves of Ti and HA-coated samples

Samples	E_{corr} (V)	I_{corr} (10^{-6} A/cm^2)	R_p ($\Omega \cdot$cm^2)	Corrosion rate (mm/year)	H (%)
Ti	0.14878	2.5756	21700	0.029928	0
HA	0.76291	0.49	61639	0.0056938	80.96

Comparable electrochemical trends have been reported in previous studies on hydroxyapatite coatings synthesized by plasma electrolytic oxidation. For example, Montazeri and Dehghanian [38] reported that HA-containing coatings prepared on Ti-6Al-4V alloys exhibited a corrosion current density of approximately 4.6×10^{-7} A/cm^2, significantly lower than that of the untreated substrate (1.7×10^{-6} A/cm^2), confirming the protective role of the PEO-derived HA layer. These values are of the same order of magnitude as the present study, where the HA coating reduces the corrosion current density to 0.49×10^{-6} A/cm^2, indicating a similar electrochemical protection level. In another study, Lan et al., [39] reported that hydroxyapatite coatings produced by the PEO process increased the corrosion potential from -0.455 V to -0.008 V, demonstrating a significant positive shift in E_{corr} and improved electrochemical stability of the coated surface, confirming that calcium-phosphate phases incorporated into the oxide layer effectively improve the corrosion resistance of metallic substrates.

The morphology of BHK cells cultured on the pure Ti substrate and HA/Ti samples after 48 and 72 hours is shown in Figure 7. In Figures 7(a-b), the Ti surface exhibits a sparse cell distribution, where cells are scattered and mostly maintain a small spindle-like shape with limited filopodia attachment. After 72 hours (Figure 7b), although the number of cells increases compared to 48 hours, the spreading and surface coverage remain limited, indicating that the Ti surface is biologically inert and not particularly favorable for strong cell adhesion and proliferation.

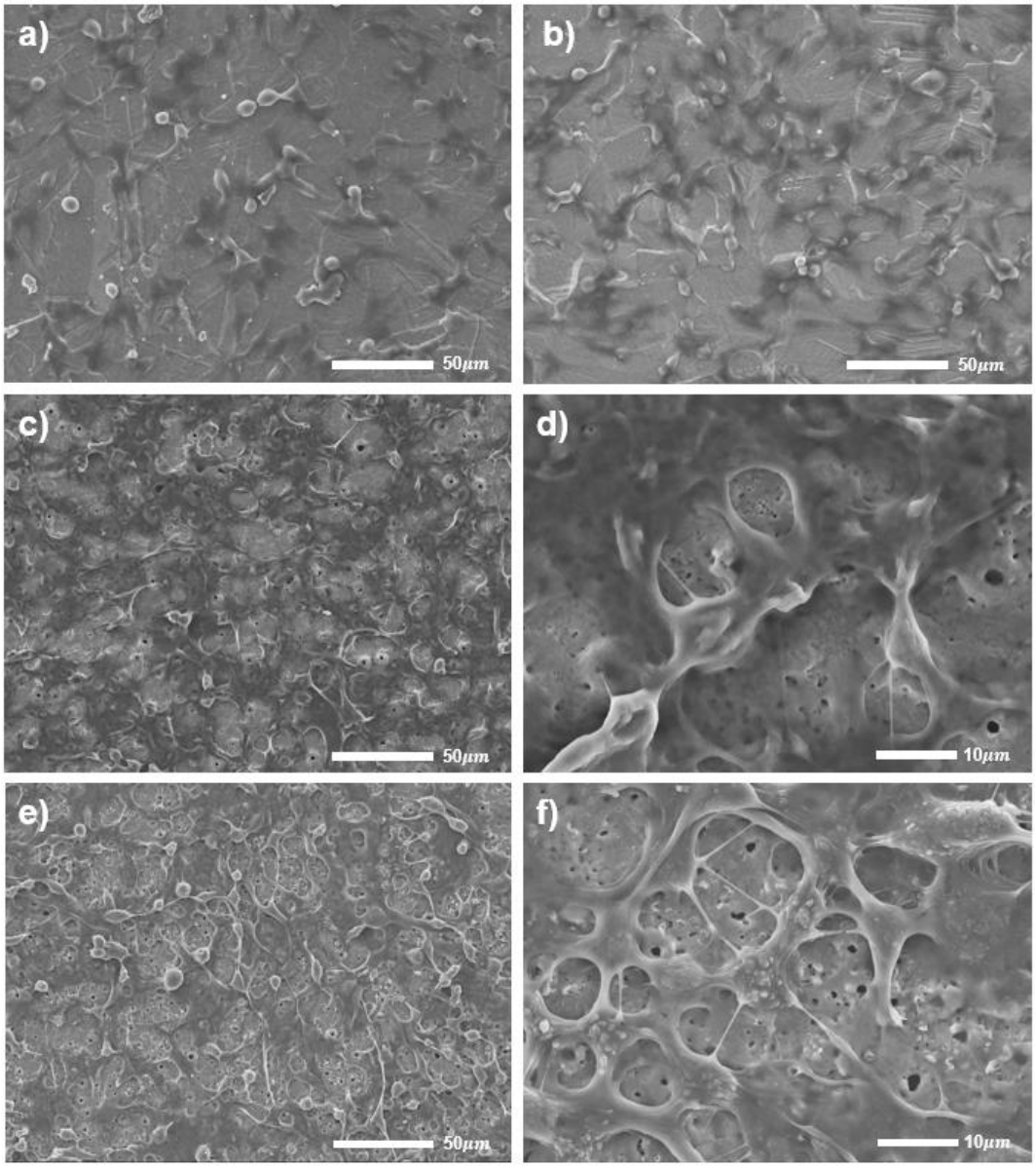


Figure 7. SEM images of BHK cells on Ti at 48h (a) and 72h (b), and on HA/Ti at 48h (c-d) and 72h (e-f).

In contrast, Figures 7(c-f) show a clear difference observed in the HA/Ti samples. As early as 48 hours (Figures 7c-d), the cell density is noticeably higher, with cells adhering in clusters and beginning to spread, forming numerous filopodia that probe and anchor to the porous HA coating surface. The magnified image (Figure 7d) reveals that cells have directly interacted with the surface and formed an interconnected network, demonstrating the HA coating's ability to support cell development. Particularly, after 72 hours (Figures 7e-f), the HA/Ti samples surface is almost completely covered by a dense cell layer, with many cells fully spread, elongated, and forming a continuous network structure. This reflects the high biocompatibility of the HA coating, allowing cells not only to adhere effectively but also to proliferate rapidly over time. Compared with the pure Ti substrate, the HA/Ti samples exhibit

superior cell density, spreading, and growth, confirming that the porous HA coating acts as a functional biological scaffold that provides a favorable environment for cell adhesion and proliferation.

4. Conclusion

In this study, hydroxyapatite (HA)-containing coatings were synthesized in situ on commercially pure titanium using plasma electrolytic oxidation (PEO) at a constant voltage of 500 V in a $Ca(CH_3COO)_2$-$NaH_2PO_4 \cdot H_2O$ electrolyte without additional post-treatment. The treatment duration significantly influenced the phase evolution of the coating. Crystalline HA was observed after 7 min of treatment, whereas shorter durations mainly produced TiO_2 phases (anatase and rutile) together with intermediate calcium phosphate phases.

The resulting HA/Ti coating exhibited a multiscale porous morphology consisting of submicron pores and larger discharge pores with diameters of approximately 2.25-3.16 μm, together with nanoscale Ca-P particulates. Energy-dispersive spectroscopy confirmed the incorporation of Ca and P species in the coating, with a Ca/P ratio of approximately 1.64, which is close to the stoichiometric value of hydroxyapatite (1.67), indicating the formation of HA-like calcium phosphate phases.

Electrochemical measurements in simulated body fluid demonstrated a positive shift in corrosion potential, a significant reduction in corrosion current density, and an increase in polarization resistance compared with untreated titanium, indicating improved corrosion resistance of the coated surface. In addition, *in vitro* BHK cell culture results showed enhanced cell adhesion and spreading on the HA/Ti coating compared with bare titanium.

Overall, these findings suggest that the PEO process can produce a porous HA-containing coating with good interfacial integrity, improved corrosion resistance, and favorable cell response. The developed HA/Ti system therefore shows potential for applications in biomedical implants.

Acknowledgments

This research is funded by Hanoi University of Science and Technology (HUST) under project number T2024-TĐ-009

References

[1] C. N. Elias, J. H. C. Lima, R. Valiev, M. A. Meyers, Biomedical Applications of Titanium and Its Alloys, JOM, Vol. 60, No. 3, 2008, pp. 46-49, https://doi.org/10.1007/s11837-008-0031-1.

[2] M. Geetha, A. K. Singh, R. Asokamani, A. K. Gogia, Ti Based Biomaterials, The Ultimate Choice for Orthopaedic Implants - A Review, Progress in Materials Science, Vol. 54, No. 3, 2009, pp. 397-425, https://doi.org/10.1016/j.pmatsci.2008.06.004.

[3] M. Long, H. J. Rack, Titanium Alloys in Total Joint Replacement - A Materials Science Perspective, Biomaterials, Vol. 19, No. 18, 1998, pp. 1621-1639, https://doi.org/10.1016/S0142-9612(97)00146-4.

[4] K. Fatehi, F. Moztarzadeh, M. S. Hashjin, M. Tahriri, M. Rezvannia, R. Ravarian, In vitro Biomimetic Deposition of Apatite on Alkaline and Heat Treated Ti6A14V Alloy Surface, Bull Mater Sci, Vol. 31, No. 2, 2008, pp. 101-108, https://doi.org/10.1007/s12034-008-0018-0.

[5] R. Halouani, D. B. Assolant, E. Champion, A. Ababou, Microstructure and Related Mechanical Properties of Hot Pressed Hydroxyapatite Ceramics, J Mater Sci: Mater Med, Vol. 5, No. 8, 1994, pp. 563-568, https://doi.org/10.1007/BF00124890.

[6] M. Ł. Kuska, P. Krawczyk, A. Martyla, W. Hedzelek, B. D. Bobkowska, Hydroxyapatite Coating on Titanium Endosseous Implants for Improved Osseointegration: Physical and Chemical Considerations, Adv Clin Exp Med, Vol. 27, No. 8, 2018, pp. 1055-1059, https://doi.org/10.17219/acem/69084.

[7] S. Kozerski, L. Pawlowski, R. Jaworski, F. Roudet, F. Petit, Two Zones Microstructure of Suspension Plasma Sprayed Hydroxyapatite Coatings, Surface and Coatings Technology, Vol. 204, No. 9-10, 2010, pp. 1380-1387, https://doi.org/10.1016/j.surfcoat.2009.09.020.

[8] R. d'Haese, L. Pawlowski, M. Bigan, R. Jaworski, M. Martel, Phase Evolution of Hydroxapatite Coatings Suspension Plasma Sprayed Using Variable Parameters in Simulated Body Fluid, Surface and Coatings Technology, Vol. 204, No. 8, 2010, pp. 1236-1246, https://doi.org/10.1016/j.surfcoat.2009.10.022.

[9] J. Wang, C. Huang, Q. Wan, Y. Chen, Y. Chao, Characterization of Fluoridated Hydroxyapatite/Zirconia Nano-Composite Coating Deposited by A Modified Electrocodeposition Technique, Surface and Coatings Technology, Vol. 204, No. 16-17, 2010, pp. 2576-2582, https://doi.org/10.1016/j.surfcoat.2010.01.042.

[10] X. Yang, B. Zhang, J. Lu, J. Chen, X. Zhang, Z. Gu, Biomimetic Ca-P Coating on Pre-Calcified Ti Plates by Electrodeposition Method, Applied Surface Science, Vol. 256, No. 9, 2010, pp. 2700-2704, https://doi.org/10.1016/j.apsusc.2009.11.004.

[11] K. Cheng, S. Zhang, W. Weng, X. Zeng, The Interfacial Study of Sol-Gel-Derived Fluoridated Hydroxyapatite Coatings, Surface and Coatings Technology, Vol. 198, No. 1-3, 2005, pp. 242-246, https://doi.org/10.1016/j.surfcoat.2004.10.024.

[12] S. Zhang, Z. Xianting, W. Yongsheng, C. Kui, W. Wenjian, Adhesion Strength of Sol-Gel Derived Fluoridated Hydroxyapatite Coatings, Surface and Coatings Technology, Vol. 200, No. 22-23, 2006, pp. 6350-6354, https://doi.org/10.1016/j.surfcoat.2005.11.033.

[13] L. H. Long, L. D. Chen, S. Q. Bai, J. Chang, K. L. Lin, Preparation of Dense β-$CaSiO_3$ Ceramic with High Mechanical Strength and HAp Formation Ability in Simulated Body Fluid, Journal of The European Ceramic Society, Vol. 26, No. 9, 2006, pp. 1701-1706, https://doi.org/10.1016/j.jeurceramsoc.2005.03.247.

[14] F. Liu, F. Wang, T. Shimizu, K. Igarashi, L. Zhao, Formation of Hydroxyapatite on Ti-6Al-4V Alloy by Microarc oxidation and Hydrothermal Treatment, Surface and Coatings Technology, Vol. 199, No. 2-3, 2005, pp. 220-224, https://doi.org/10.1016/j.surfcoat.2004.10.146.

[15] B. C. Wang, E. Chang, T. M. Lee, C. Y. Yang, Changes in Phases and Crystallinity of Plasma-Sprayed Hydroxyapatite Coatings Under Heat Treatment: A Quantitative Study, J. Biomed. Mater. Res., Vol. 29, No. 12, 1995, pp. 1483-1492, https://doi.org/10.1002/jbm.820291204.

[16] I. M. O. Kangasniemi, C. C. P. M. Verheyen, E. A. Van Der Velde, K. De Groot, In vivo Tensile Testing of Fluorapatite and Hydroxylapatite Plasma-Sprayed Coatings, J. Biomed. Mater. Res., Vol. 28, No. 5, 1994, pp. 563-572, https://doi.org/10.1002/jbm.820280506.

[17] F. Liu, F. Wang, T. Shimizu, K. Igarashi, L. Zhao, Hydroxyapatite Formation on Oxide Films Containing Ca and P by Hydrothermal Treatment, Ceramics International, Vol. 32, No. 5, 2006, pp. 527-531, https://doi.org/10.1016/j.ceramint.2005.04.006.

[18] G. Li et al., Review of Micro-Arc Oxidation of Titanium Alloys: Mechanism, Properties and Applications, Journal of Alloys and Compounds, Vol. 948, 2023, pp. 169773, https://doi.org/10.1016/j.jallcom.2023.169773.

[19] A. L. Yerokhin, X. Nie, A. Leyland, A. Matthews, Characterisation of Oxide Films Produced by Plasma Electrolytic Oxidation of A Ti-6Al-4V Alloy, Surface and Coatings Technology, Vol. 130, No. 2-3, 2000, pp. 195-206, https://doi.org/10.1016/S0257-8972(00)00719-2.

[20] S. Durdu, Ö. F. Deniz, I. Kutbay, M. Usta, Characterization and Formation of Hydroxyapatite on Ti6Al4V Coated by Plasma Electrolytic Oxidation, Journal of Alloys and Compounds, Vol. 551, 2013, pp. 422-429, https://doi.org/10.1016/j.jallcom.2012.11.024.

[21] A. F. Alhosseini, R. Chaharmahali, M. K. Keshavarz, K. Babaei, Surface Characterization of Bioceramic Coatings on Zr and Its Alloys Using Plasma Electrolytic Oxidation (PEO): A Review, Surfaces and Interfaces, Vol. 25, 2021, pp. 101283, https://doi.org/10.1016/j.surfin.2021.101283.

[22] B. M. Kasprolewicz, A. Ossowska, Recent Advances in Electrochemically Surface Treated Titanium and Its Alloys for Biomedical Applications: A Review of Anodic and Plasma Electrolytic Oxidation Methods, Materials Today Communications, Vol. 34, 2023, pp. 105425, https://doi.org/10.1016/j.mtcomm.2023.105425.

[23] F. Hafili, R. Chaharmahali, K. Babaei, A. F. Alhosseini, Duty Cycle Influence on the Corrosion Behavior of Coatings Created by Plasma Electrolytic Oxidation on AZ31B Magnesium Alloy in Simulated Body Fluid, Corrosion Communications, Vol. 3, 2021, pp. 62-70, https://doi.org/10.1016/j.corcom.2021.09.005.

[24] E. Mohammadipour, M. Ghorbani, Characterization, Mechanical, Corrosion, and in vitro Apatite-Formation Ability Properties of Hydroxyapatite-Reduced Graphene Oxide Coatings on Ti6Al4V Alloy by Plasma Electrolytic Oxidation, Journal of Materials Research and Technology, Vol. 33, 2024, pp. 441-457, https://doi.org/10.1016/j.jmrt.2024.09.041.

[25] S. Durdu, K. Korkmaz, S. L. Aktuğ, A. Çakır, Characterization and Bioactivity of Hydroxyapatite-Based Coatings Formed on Steel by Electro-Spark Deposition and Micro-Arc Oxidation, Surface and Coatings Technology, Vol. 326, 2017, pp. 111-120, https://doi.org/10.1016/j.surfcoat.2017.07.039.

[26] L. Li, H. Kim, S. Lee, Y. Kong, H. Kim, Biocompatibility of Titanium Implants Modified by Microarc Oxidation and Hydroxyapatite Coating, J Biomedical Materials Res, Vol. 73A, No. 1, 2005, pp. 48-54, https://doi.org/10.1002/jbm.a.30244.

[27] V. S. Rudnev, V. P. Morozova, I. V. Lukiyanchuk, M. V. Adigamova, Calcium-Containing Biocompatible Oxide-Phosphate Coatings on Titanium, Russ J Appl Chem, Vol. 83, No. 4, 2010, pp. 671-679, https://doi.org/10.1134/S107042721004018X.

[28] W. H. Song, Y. K. Jun, Y. Han, S. H. Hong, Biomimetic Apatite Coatings on Micro-Arc Oxidized Titania, Biomaterials, Vol. 25, No. 17, 2004, pp. 3341-3349, https://doi.org/10.1016/j.biomaterials.2003.09.103.

[29] H. Cimenoglu, M. Gunyuz, G. T. Kose, M. Baydogan, F. Uğurlu, C. Sener, Micro-Arc Oxidation of Ti6Al4V and Ti6Al7Nb Alloys for Biomedical Applications, Materials Characterization, Vol. 62, No. 3, 2011, pp. 304-311, https://doi.org/10.1016/j.matchar.2011.01.002.

[30] D. Wei, Y. Zhou, D. Jia, Y. Wang, Structure of Calcium Titanate/Titania Bioceramic Composite Coatings on Titanium Alloy and Apatite Deposition on Their Surfaces in A Simulated Body Fluid, Surface and Coatings Technology, Vol. 201, No. 21, 2007, pp. 8715-8722, https://doi.org/10.1016/j.surfcoat.2007.04.124.

[31] A. Yerokhin, E. V. Parfenov, A. Matthews, In situ Impedance Spectroscopy of The Plasma Electrolytic Oxidation Process for Deposition of Ca- and P-Containing Coatings on Ti, Surface and Coatings Technology, Vol. 301, 2016, pp. 54-62, https://doi.org/10.1016/j.surfcoat.2016.02.035.

[32] J. Sun, Y. Han, X. Huang, Hydroxyapatite Coatings Prepared by Micro-Arc Oxidation in Ca- and P-Containing Electrolyte, Surface and Coatings Technology, Vol. 201, No. 9-11, 2007, pp. 5655-5658, https://doi.org/10.1016/j.surfcoat.2006.07.052.

[33] T. T. An et al., Corrosion Resistance of Zinc-Doped Hydroxyapatite Coating on Titanium Substrate Using Plasma Electrolytic Oxidation for Biomedical Applications, J. of Materi Eng and Perform, Vol. 34, No. 8, 2025, pp. 6743-6754, https://doi.org/10.1007/s11665-024-09636-8.

[34] V. Karageorgiou, D. Kaplan, Porosity of 3D Biomaterial Scaffolds and Osteogenesis, Biomaterials, Vol. 26, No. 27, 2005, pp. 5474-5491, https://doi.org/10.1016/j.biomaterials.2005.02.002.

[35] C. H. Huang, M. Yoshimura, Direct Ceramic Coating of Calcium Phosphate Doped with Strontium Via Reactive Growing Integration Layer Method on α-Ti Alloy, Sci Rep, Vol. 10, No. 1, 2020, pp. 10602, https://doi.org/10.1038/s41598-020-67332-8.

[36] S. Arun, S. G. Ahn, H. C. Choe, Surface Characteristics of HA-Coated and PEO-Treated Ti-6Al-4V Alloy in Solution Containing Ag Nanoparticles, Surfaces and Interfaces, Vol. 39, 2023, pp. 102932, https://doi.org/10.1016/j.surfin.2023.102932.

[37] E. Lokeshkumar et al., Development of TiO_2-HA Coatings by PEO on Titanium Scaffolds Fabricated by Direct Ink Writing, Trans Indian Inst Met, Vol. 76, No. 2, 2023, pp. 511-518, https://doi.org/10.1007/s12666-022-02714-2.

[38] M. Montazeri, C. Dehghanian, M. Shokouhfar, A. Baradaran, Investigation of the Voltage and Time Effects on the Formation of Hydroxyapatite-Containing Titania Prepared by Plasma Electrolytic Oxidation on Ti-6Al-4V Alloy and Its Corrosion Behavior, Applied Surface Science, Vol. 257, No. 16, 2011, pp. 7268-7275, https://doi.org/10.1016/j.apsusc.2011.03.103.

[39] L. Zhou, G. H. Lü, F. F. Mao, S. Z. Yang, Preparation of Biomedical Ag Incorporated Hydroxyapatite/Titania Coatings on Ti6Al4V Alloy by Plasma Electrolytic Oxidation, Chinese Phys. B, Vol. 23, No. 3, 2014, pp. 035205, https://doi.org/10.1088/1674-1056/23/3/035205.